SAND2015-2114C

Residual internal stress optimization for EPON 828/DEA thermoset resin using fiber Bragg grating sensors

Garth D. Rohr*[a], Roger D. Rasberry[a], Amy K. Kaczmarowksi[a], Mark E. Stavig[a], Cory S. Gibson[b], Eric Udd[b], Allen R. Roach[a], Brendan Nation[a]
[a]Sandia National Laboratories, P. O. Box 5800, MS 0888, Albuquerque, NM, USA 87185-0888
[b]Columbia Gorge Research, LLC, P. O. Box 382, 2555 NE 205th Ave, Fairview, OR USA 97024

ABSTRACT

Internal residual stresses and overall mechanical properties of thermoset resins are largely dictated by the curing process. It is well understood that fiber Bragg grating (FBG) sensors can be used to evaluate temperature and cure induced strain while embedded during curing. Herein, is an extension of this work whereby we use FBGs as a probe for minimizing the internal residual stress of an unfilled and filled Epon 828/DEA resin. Variables affecting stress including cure cycle, mold (release), and adhesion promoting additives will be discussed and stress measurements from a strain gauge pop-off test will be used as comparison.

Sandia National Laboratories is a multi-program laboratory managed and operated by Sandia Corporation, a wholly owned subsidiary of Lockheed Martin Corporation, for the U.S. Department of Energy's National Nuclear Security Administration under contract DE-AC04-94AL85000.

Keywords: Fiber Bragg grating, chirped, stress, epoxy, encapsulation, cure

1. INTRODUCTION

Epoxy resins are used to encapsulate and protect a variety of sensitive electronic equipment. These encapsulation systems are often chosen for their unique and highly advantageous final properties such as fracture toughness, dielectric constant, and coefficient of thermal expansion. However, in the determination of an appropriate encapsulation system, often considerably less attention is given to the path by which the systems develop these desirable final properties. The cure kinetics of epoxy encapsulation systems are typically explored separately from the system of interest due to the limitations of available experimental methods. This can often cause unanticipated and undesirable stresses to develop between the electronic components and the encapsulation system during cure. Such stresses can lead to poor adhesion between the component and encapsulation and ultimately system failures.[1-3]

As encapsulation systems cure, the cross-linking reaction causes shrinkage in the material that can produce added stresses to the encapsulated component and the component interfaces. Typically, measures are taken to utilize non-isothermal cure profiles that attempt to balance the chemical cure shrinkage with the thermal expansion of the epoxy to reduce the overall impact on the system. However, these cure profiles are often developed either using small volumes of epoxies studied through techniques such as differential scanning calorimetry or infrared, which focus on accurate measurements and models of the cure kinetics, or using overly simplified geometries that allow for the use of strain gauges mounted to thin-walled embedded components. Yet these techniques do not allow for an understanding of stresses that may develop in the multi-faceted features of many electronic components.

Several recent advances have been made in the use of embedded fiber optic sensors for analyzing the development of stresses during the cure of epoxies in complex systems. Such sensors can help to bridge the gap between standard cure kinetics studies and the application of these systems to real world components. Fiber Bragg gratings (FBG) are often embedded into the bulk polymer matrix to measure stresses generated during encapsulation, cure shrinkage, extent of reaction, etc.[4-8] Herein, we have set out to utilize the fiber optic sensors to monitor areas of high stresses near an encapsulated component and identify how those stresses change in response to alterations in the cure profile and as a result of interactions between multiple encapsulation systems.

1.1 Background

The fiber Bragg grating sensor diagnostic is shown in Figure 1 and can be described as follows.[9-11] An typical fiber optic cable is exposed to UV light using a phase mask or via holographic techniques. The light changes the local refractive index of the exposed glass regions thereby inducing a pattern. The pattern can be uniform (periodic) along the entire length of the exposed portion of the fiber or graduated (chirped) such that the spacing in the grating is smaller on one end and larger on the other. The length of the grating typically ranges from a couple millimeters to over one hundred.

When light from a superluminescent LED lightsource is directed into a chirped fiber, most of the light is transmitted except for a broadband spectral reflectance peak (usually 1535-1560 nanometers) corresponding to the grating spacing. Any change in the grating spacing affects the reflected light, which is referred to as the reflected Bragg signal. For example, when the fiber grating is under tension, the reflected signal will shift to longer wavelengths. Likewise, when the fiber is under compression the signal will shift to shorter wavelengths. A non-uniform stress applied anywhere along the length of the chirped grating will affect the reflected signal at that location. Thus, it is possible to get local information about compression (or a lack thereof) at a particular point along the grating. The more common FBGs with a periodic spacing work similarly but, since the grating spacing is uniform, local changes are not as discernable compared to chirped FBGs.

To determine the efficacy of both types of fibers for monitoring stresses near component interfaces, fibers were incorporated into aluminum molds and encapsulated using a well characterized epoxy system. Various cure profiles were used to measure stressing during curing, cooling, and subsequent thermal cycling.[9]

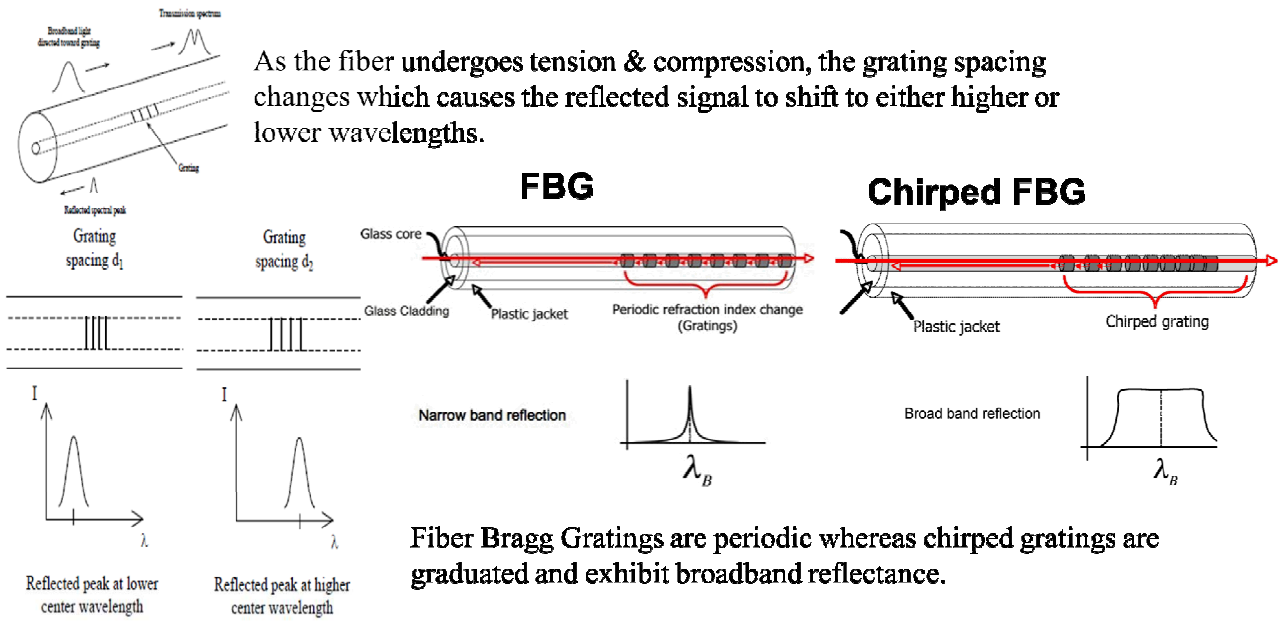

Figure 1. Fiber Bragg grating system; changes in the grating spacing translate into shifts in the reflected Bragg signal.

2. EXPERIMENTAL

2.1 FBG System

The fiber optic setup consisted of a Denselight DL-BP1-1501A Superluminescent LED Source (with Integrated Optical Circulator) and an I-MON 512E-USB 2.0 Interrogation Monitor. Two Micron Optics systems were also used which consisted of a sm125-500 (4-Ch, 80nm Wvl Range, 2Hz Scan, 1pm Wvl Acc, 1pm Wvl Stab, 0.5pm Wvl Repeat @ 1Hz, 50dB DR, ENLIGHT) and si225-500 (8-Ch, 160nm Wvl Range, 1kHz Scan, 1pm Wvl Acc, 1pm Wvl Stab, 1pm Wvl Repeat, 20dB DR). Fiber sensors consisted of the os1100 FBG from Micron Optics and four different custom-made chirped FBGs manufactured by Timbercon, Inc and O/E Land Inc. Each of the custom chirped FBGs were polyimide

coated and had a central wavelength of ~1547-1548 nm. The only variance was in the reflectivity (40-50%) and grating length (10 or 12 mm).

2.2 Chemicals

Epon 828 resin was purchased from Miller-Stephenson, diethanolamine (DEA) curing agent was purchased from Acros Organics, Epon 826 was purchased from EV Roberts, CTBN was purchased from Honeywell FM&T and glass microballoons (D32) were purchased from 3M. Fibers were attached to molds using either EPO-TEK 353ND or Norland electronic Adhesive 121. Frekote 44-NC mold release from Henkel was also used in this work.

2.3 Molds

Two aluminum mold geometries were used in these experiments (Figure 2). The first was a cylinder (1" x 3.5") machined from aluminum that has a replaceable thin disk on the bottom which is referred to as the "pop-off" mold. The inside walls were roughened by a sand blaster to promote adhesion. A second, more complex geometry was also used whereupon the inside of the mold was polished and treated with Freekote 44-NC so that the epoxy assembly could then be removed.

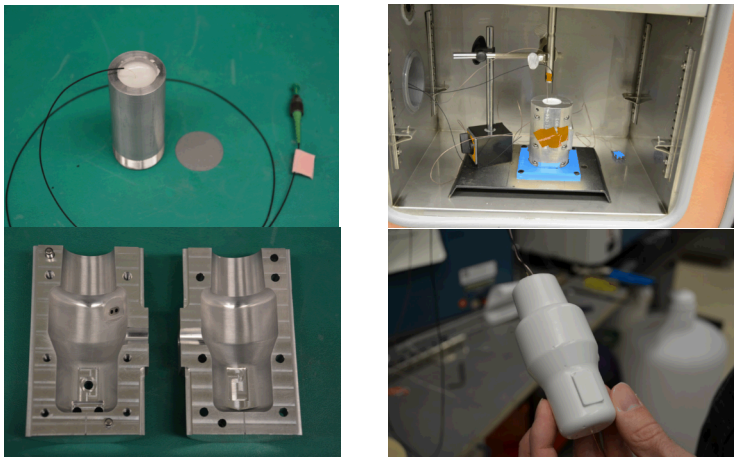

Figure 2. Simple pop-off mold geometry (top left) and the fiber embedding process using a complex mold.

2.4 Processing

Epon 828, Epon 826, CTBN, and DEA were pre-heated for 2 hours at 71°C while the glass microballoons (GMB) were pre-heated at 107 °C. For the 828/GMB/DEA epoxy mixture, Epon 828 was mixed with the glass microballoons until wetted and then DEA was added and stirred by hand for 5 minutes. Alternatively, for the 826/CTBN/DEA epoxy, Epon 826 was mixed with CTBN and then mixed by hand with the DEA for 5 minutes. The mixture was degassed (2 torr, 71 °C) for a sufficient amount of time to remove the majority of air introduced by mixing and then poured into the molds. The epoxy was cured in an oven using one of three two-tier cure profiles with an intermediate isothermal stage followed by thermal ramp to 71 °C and then a slow cool to room temperature. The first cure profiles, referred to as the 27hr cure and the 29hr cure, differ in that there is an additional 2 hours at the intermediate isothermal stage for the 29hr cure profile. The third cure profile, referred to as the 56hr cure profile, has a 10°C lower temperature during the isothermal hold. This requires a much longer hold time relative to the other two cures in order to achieve the same final cure state as the other cure profiles. All three cures had the same ramp rate to 71°C, length of hold at this temperature, and cool down rate.

3. RESULTS AND DISCUSSION

We first set out to evaluate the FBG using a simple pop-off tube geometry so that the FBG signal could be compared a strain measurement taken from a strain gauge affixed to a thin disk on the bottom of the mold. We utilized the pop-off tube to measure the stress generated in the bulk epoxy using the os1100 FBG and sm125 interrogator as well as an Omega SGD-3/350-LY13 strain gauge. It was impossible to simultaneously measure strain using both techniques

because the FBG was tacked vertically through the cylinder mold to the thin disk at the bottom, which would have interfered with the strain gauge data. As such, we used separate pop-off tubes for each method each with equal amounts of epoxy. Results for these two tube tests are shown in Figure 3. The reflected Bragg signal remains constant until the polymer begins to gel, which is also evident for the thin disk strain gauge. The gel point is reached when the modulus of the reacting epoxy is high enough to induce a measureable strain on the fiber grating. We have approximated this minimum modulus to be approximately 10 MPa. The epoxy shrinks as it crosslinks and the modulus begins to grow until ultimately imparting a strain (compression) on the fiber. During temperature ramping, thermal expansion of the cross-linked polymer begins to dominate leading to relaxation of the compressed grating. Interestingly, the gel point is detected 3 ½ hours earlier with the FBG versus the thin disk strain gauge. This suggests that the FBG is more sensitive to modulus evolution & cure shrinkage of the cross-linking polymer.

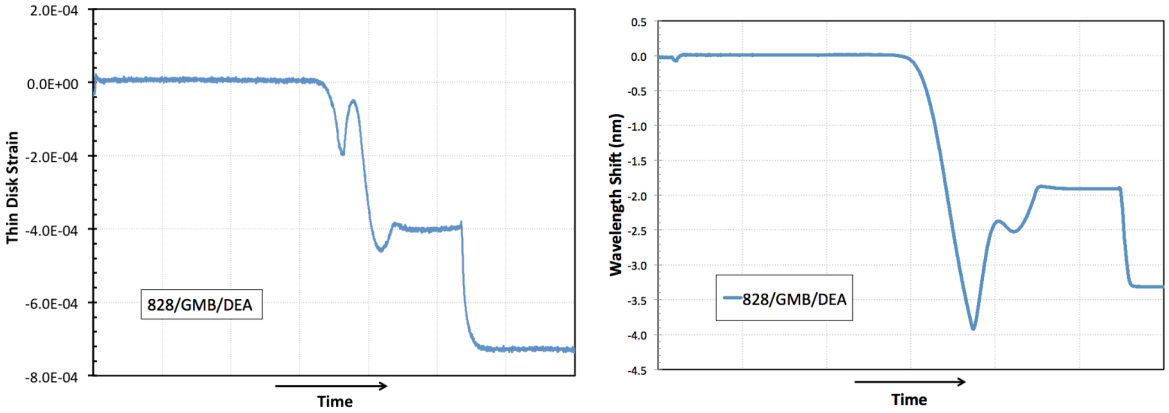

Figure 2. 56 hour strain gauge data (left) and FBG response (right).

An alternative 27 hr cure profile was then evaluated in the more complex geometry filled with 828/GMB/DEA epoxy such that it could be removed from the aluminum mold and temperature cycled. An FBG was encapsulated vertically at the center point of the mold. The gel point occurs during the second thermal ramp so there is competition between cure shrinkage and expansion due to the increasing temperature and coefficient of thermal expansion (CTE) of the polymer. After reaching a minimum, the matrix begins to expand and then plateaus during the high temperature isothermal portion of the cure schedule. The temperature is then cooled to room temp where the thermal stresses impart a large strain onto the polyimide coating fiber which is known to have excellent strain transfer efficiency in epoxy thermoset resins such as this.[12] Ultimately, the fiber experiences a total compression of 4.7 nm which corresponds to a strain value 5620 με.

Oftentimes, thermoset resins are thermally annealed to relieve internal residual stresses. These stresses occur when there is poor release from the encapsulant/mold during cooling to room temperature at the end of cure. One of the great advantages of the fiber Bragg gratings is that they can be used to measure this strain release and also any strain relief that might occur due to the demolding process. The results in Figure 4 highlight both of these capabilities though it was found that there was very little change after demolding suggesting that the mold release was working well for this system. During the first step (on cold) of thermal cycling, the change in wavelength was small relative to values for 2 subsequent cycles which were essentially the same. The sample then sat for 1 month and was thermally cycled again but no discernable change was observed in the reflected Bragg signal after time. This is consistent with the notion that any internal residual stress was released (on hot) during the first cycle which served as a thermal annealing step.

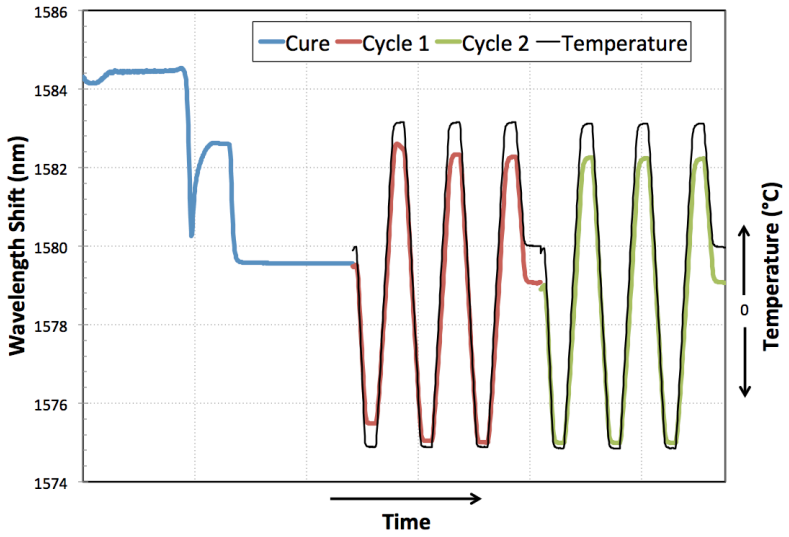

Figure 4. 27 hr cure in complex mold geometry and subsequent temperature cycling.

The gel point for the 27 hour cure schedule was observed to occur during the ramp of the cure profile. This is non-ideal for a production process as fluctuations in oven temperature could cause variability in the timing and temperature of the gel point. Since the gel point is the point at which the epoxy solidifies enough to form stress and strains, any variability in the temperature at gel point can result in systems with differing stress states and likelihood of failure. Ideally a production process would limit such unit-to-unit variability.

Parallel strain gauge thin disk pop-off tests showed that extending the cure for 2 hours could lead to isothermal gelling and as much as a 10-20 percent stress reduction in the encapsulant. As such, we set out to determine what effect this extended cure would have on a fiber optic in the complex mold geometry. One additional variable was the incorporation of a second epoxy system such that ½ of the mold would be filled with 826/CTBN/DEA and the top portion would consist of 828/GMB/DEA. The chirped FBG (40-50%, 10 mm) was then placed in the center of the mold perpendicular to the interface of this binary encapsulant system. Results are shown in Figure 5.

Unfortunately, an insufficient amount of 826/CTBN/DEA was used in the 27 hour cure so the chirped FBG only experienced strain from the 828/GMB/DEA. This resulted in a -7.2 nm shift on the short wavelength end of the grating and a -6.3 nm shift on the long wavelength end. In the case of a 29 hr cure, the chirped FBG experienced strain from both systems of epoxy resulting in a shift of -5.1 nm from the 828/GMB/DEA and -7.3 nm shift from the 828/CTBN/GMB. The reduction of the cure induced compression in the 29 hr for the Epon 828/GMB/DEA in comparison to the 27 hr cure indicates that gelation prior to thermal ramping is important to reducing stress in the cured encapsulant.

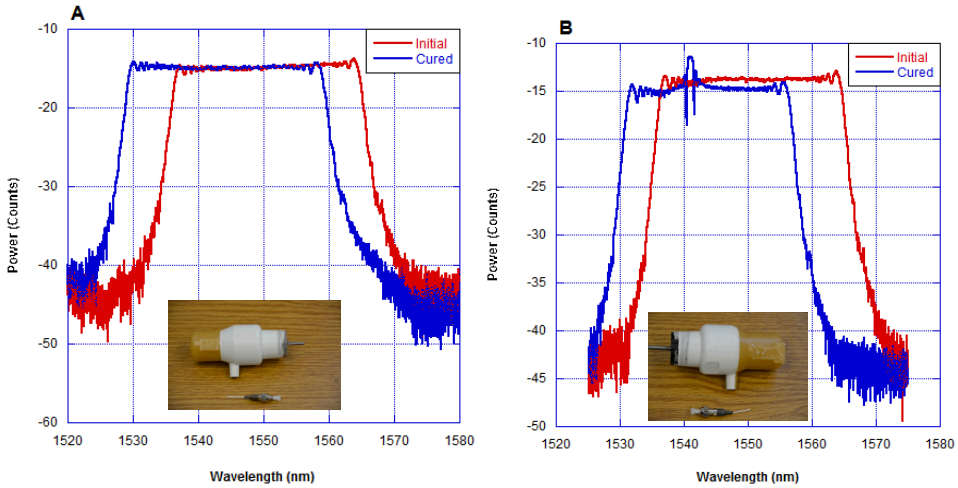

Figure 5. A) Chirped FBG reflected signal for the 27 hr cure. B) Chirped FBG reflected signal for the 29 hr cure.

Previous pop off tube experiments with 828/GMB/DEA had shown that stresses could be reduced by as much as 50% if the temperature was reduced by 10 degrees and extended to 56 hours. As such, we next set out to investigate this cure profile in the complex mold with binary encapsulant. This experiment was carried out in the same manner as that for figure 5 by threading the fiber through the interface of the 828/GMB/DEA and 826/CTBN/DEA. Interestingly, the short wavelength end of the chirped grating which extends into the 828/GMB/DEA was under tension (2.1 nm, 2520 με) whereas the opposite end of the fiber which is surrounded by 826/CTBN/DEA was underwent compression (-4.6 nm, 5520 με) at the end of cure/cooling (Figure 6). Though this experiment was repeated several times, the same result was achieved each time so it appears that very different behavior is occurring at the interface during the 56 hr versus the 27 and 29 hr schedules. Thus, stress reduction in an isolated encapsulant does not necessarily translate to the same output for a binary system in a complex geometry. It is not clear whether the 828/GMB/DEA under tension at the interface is good or bad at this point. We are currently working to define the advantages and disadvantages of this phenomenon.

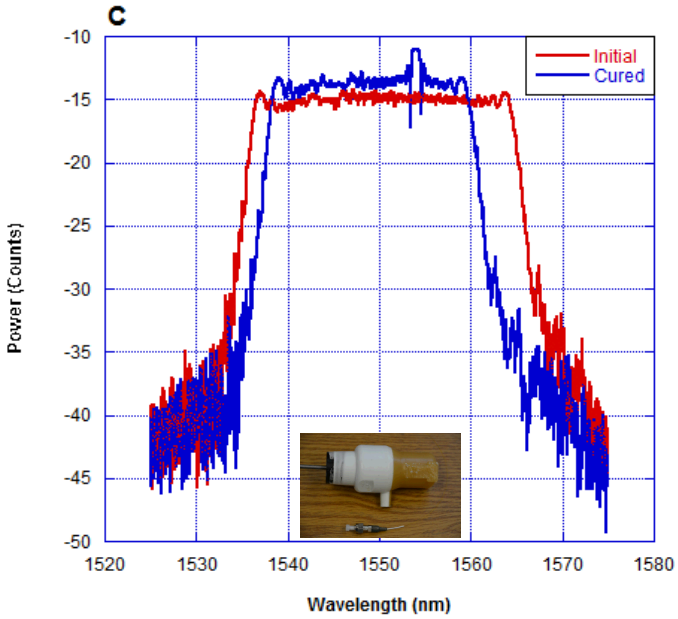

Figure 6. Chirped FBG reflected signal for the 56 hr cure.

One possible explanation for the behavior observed for the 56 hour cure is that the 826/CTBN/DEA was swelling and expanding into the 828/GMB/DEA (which gels at a later point) and during cooling the 826/CTBN/DEA shrinks and puts

the 828/GMB/DEA under tension. To verify if this was possible, a pop-off test was carried out for the 826/CTBN/DEA using the 56 hour cure schedule with results shown in Figure 7. The blue curve corresponds to a pop-off tube containing 828/GMB/DEA and the red curve is for a pop-off tube filled with 826/CTBN/DEA. The results of the fiber responses clearly show that the 826/CTBN/DEA swells whereas the 828/GMB/DEA does not for this cure profile which is consistent with the notion that the 826/CTBN/DEA is swelling more during this profile and ultimately placing the 828/GMB/DEA in tension at the interface during cooling in this bimodal filled complex geometry. Perhaps the stresses in the 828/GMB/DEA are different further away from the interface and in the bulk. We are in the process of investigating this now by embedding a fiber away from the interface and near an encapsulated object.

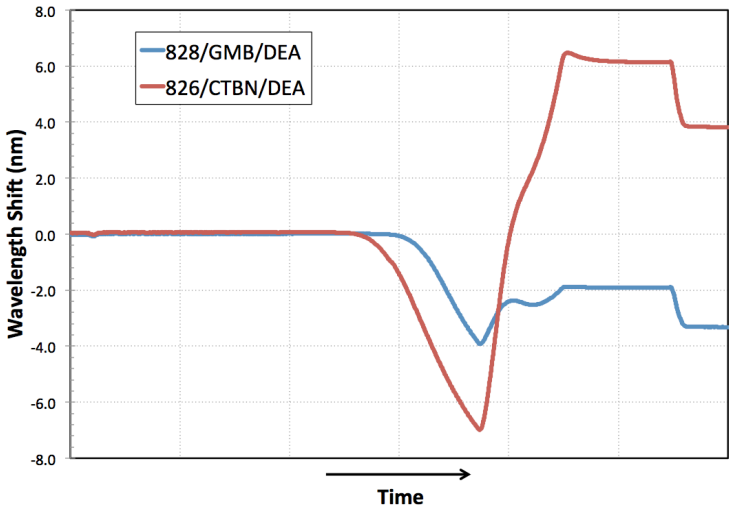

Figure 7. FBG data conducted in pop-off tubes.

4. CONCLUSIONS

Fiber optic Bragg grating sensing technology can have an enormous impact in the area of reducing internal residual stress in bulk epoxy systems. The ability to provide *in situ* information about stresses generated during various cure profiles is incredible and threading a fiber through the interface of binary encapsulant system in complex mold geometries highlights the utility of this approach. We are currently working to develop a model to help define the fiber optic response at different locations in the mold as well as continuing to look at reducing internal residual stress by changing processing parameters such as cure profile.

REFERENCES

[1] Chambers, R. S.; Lagasse, R. R.; Guess, T. R.; Plazek, D. J.; Bero, C. *Journal of Electronic Packaging* **1995**, *117*, 249.
[2] Adolf, D. B.; Stavig, M. E.; Kawaguchi, S.; Chambers, R. S. *J. Adhes.* **2007**, *83*, 85.
[3] Adolf, D. B.; Chambers, R. S.; Hance, B.; Elisberg, B. *J. Adhes.* **2010**, *86*, 1111.
[4] Giordano, M.; Laudati, A.; Nasser, J.; Nicolais, L.; Cusano, A.; Cutolo, A. *Sens. Actuator A-Phys.* **2004**, *113*, 166.
[5] Harsch, M.; Karger-Kocsis, J.; Herzog, F. *Macromolecular Materials and Engineering* **2007**, *292*, 474.
[6] Wang, Y.; Han, B.; Kim, D. W.; Bar-Cohen, A.; Joseph, P. *Exp. Mech.* **2008**, *48*, 107.
[7] Case, S. L.; O'Brien, E. P.; Ward, T. C. *Polymer* **2005**, *46*, 10831.
[8] Cusano, A.; Capoluongo, P.; Cutolo, A.; Giordano, M. *IEEE Sens. J.* **2006**, *6*, 111.
[9] Kashyap, R. *Fiber Bragg Gratings (Second Edition)*; Academic Press, 2010.
[10] Measures, R. M. *Structural Monitoring with Fiber Optic Technology*; Academic Press, 2001.
[11] Udd, E. *Proc. IEEE* **1996**, *84*, 60.
[12] Difrancia, C.; Claus, R.; Hellgeth, J. W.; Ward, T. C. *STRUCTURE PROPERTY CORRELATIONS OF SEVERAL POLYIMIDE OPTICAL FIBER COATINGS FOR EMBEDDING IN AN EPOXY MATRIX*; Spie - Int Soc Optical Engineering: Bellingham, 1990; Vol. 1170.